Plasma Response to Resonant Magnetic Perturbations in Large Aspect Ratio Tokamaks

André Carlos Fraile Jr., Marisa Roberto, Iberê Luiz Caldas, and Caroline Gameiro Lopes Martins

***Abstract*— In this paper, a plasma response model is investigated for large aspect ratio tokamaks, on the presence of external nonaxisymmetric resonant magnetic perturbations. To control plasma confinement, the plasma is perturbed by external resonant helical windings, similar to those introduced by an ergodic magnetic limiter. The plasma response to the perturbation is modeled as an additional magnetic perturbation, created by a current sheet on the main perturbed resonant surface, vanishing the radial component of the total magnetic field in the considered resonant surface. In order to show the influence of the plasma response on the field line topology, the field line differential equations are integrated numerically, showing the reduction of magnetic island sizes and the regularization of chaotic regions around the resonant surface where the response was introduced, in agreement with results observed in sophisticated simulation codes. Finally, the connection lengths indicate that, regarding their distribution, the plasma response introduces a homogenization effect which may affect the deposition patterns at the tokamak wall.**

***Index Terms*— Plasma response, resonant magnetic perturbation (RMP), tokamak.**

I. Introduction

HIGH temperature particles at the edge of magnetically confined plasmas, such as tokamaks, collide with neutral gas, material surfaces, and the associated impurities. The transport of heat and particles in this region determines the heat loads and erosion rates of plasma facing components [1]. If the heat and particle loadings are spatially localized, the sputtering processes, occurring on the wall, releases impurities into the plasma column, deteriorating the overall confinement quality [2]. Different kinds of coils have been used to modify the spatial distribution of the particles and heat transport at the tokamak border in order to improve the plasma confinement. Examples of these coil sets are the resonant helical windings and the ergodic magnetic limiter (EML) applied to create resonant magnetic perturbations (RMPs) at the plasma edge [3]–[11].

The resonant helical windings create an externally induced perturbation of the equilibrium magnetic field, which resonates at a given magnetic flux surface position, usually located in the plasma edge. It resonates because the perturbation has the same helicity as the equilibrium magnetic field at a target flux surface. The perturbation leads to chaotic magnetic field lines around the resonant flux surface, generating a chaotic layer near the tokamak wall [12]. However, the plasma itself is capable of modifying the magnetic perturbation field and, for some parameters, the plasma response may modify significantly the effective perturbation amplitude [13]–[15].

The plasma response determines the actual perturbation field inside the plasma, which can differ from the one it would have in the vacuum. The change of RMP field by the plasma response has been considered theoretically [16]–[19] and experimentally [20], [21], still requiring additional studies to understand its effects on the magnetic field structure in tokamaks [22]. It has been pointed out that the generated magnetic islands can be modified since the plasma is able to screen the resonant modes of the perturbation, giving rise to different results from those ones predicted by the vacuum perturbation approach. It is important to know whether the resonant perturbation, in the RMP experiments, penetrates or get screened, in order to elucidate relevant effects such as ELM suppression [15], [23], [24] and density pump out [25]. A model of the plasma response field, created by a rotating tearing instability, shows that the measured heat flux to the divertor plates of a single-null discharge, at the DIII-D tokamak, evolves in agreement with the interior of a rotating invariant manifold [26]. This approach has shown that modeling the plasma response as a result of perturbation currents can be effective to analyze a region of the DIII-D tokamak that would otherwise require a complex study of resistive magnetohydrodynamics [26]. Therefore, predicting the plasma response to the external RMP fields clarifies the resulting magnetic topology at the plasma edge, determining plasma transport and thermal depositions at the plasma wall [27]. Understanding the plasma response in analytical models may contribute to both the ITER experiment, currently under construction, and DEMO, the first demonstration reactor.

In this paper, a large aspect ratio tokamak in equilibrium is modified by the presence of nonaxisymmetric RMPs, similar to thoseintroduced by an EML. Following [14], the plasma response is modeled by a current sheet, vanishing the radial component of the total magnetic field on the main resonant

Manuscript received May 11, 2017; revised August 23, 2017; accepted October 2, 2017. Date of publication October 17, 2017; date of current version November 8, 2017. This work was supported in part by São Paulo Research Foundation, FAPESP, Brazil, under Grant N° 2015/16471-8 and Grant 2011/19296-1, in part by CNPq, Brazil, under Grant N° 446905/2014-3, and in part by CAPES, Brazil. The review of this paper was arranged by Senior Editor A. I. Smolyakov. *(Corresponding author: Marisa Roberto.)*

A. C. Fraile Jr., is with the Departmento de Física, Instituto Tecnológico de Aeronáutica, São José dos Campos 12228-900, Brazil, and also with the Departamento de Aerotermodinâmica e Hipersônica, Instituto de Estudos Avançados, São José dos Campos 12228-001, Brazil (e-mail: andrecfj@gmail.com).

M. Roberto and C. G. L. Martins are with the Departmento de Física, Instituto Tecnológico de Aeronáutica, São José dos Campos 12228-900, Brazil. (e-mail: marisar@ita.br; carolinegameiro@gmail.com).

I. L. Caldas is with the Departamento de Física Aplicada, Instituto de Física, Universidade de São Paulo, São Paulo 05315-970, Brazil (e-mail: ibere@if.usp.br).

Color versions of one or more of the figures in this paper are available online at http://ieeexplore.ieee.org.

Digital Object Identifier 10.1109/TPS.2017.2760632

surface. More specifically, helical current sheets are introduced in order to mimic a hypothetical screening of the external RMP by the plasma [14]. The assumption of complete screening is justified when a strong pressure gradient suppress the resonant modes in the pedestal region [14]. We have considered here, in a first approximation, the plasma response acting only in a single rational surface, near the plasma edge. In fact, according to [14] and [15], the size of the magnetic footprints depends on the number of screening surfaces as shown for JET and COMPASS, decreasing if more screening surfaces are included. However, a single screening surface can already modify significantly the footprint size as well as the beginning of the open field line region or the field line escaping. These helical currents eliminate the magnetic islands at the resonant surface and also simulate the effects of plasma response in some experiments resulting in a stochastic layer with smaller width than predicted by vacuum calculations [28]. The condition to mitigate magnetic islands is expressed as canceling out the radial component of magnetic field at the resonant surface. Although this hypothesis has not been completely justified, it can be used to mimic the plasma response in tokamaks when the complete suppression of resonant modes is supposed near the plasma edge [14]. The magnetic field line differential equations are solved numerically in order to analyze the influence of the plasma response on the field line topology, observing the reduction of magnetic island sizes and the regularization of chaotic regions around the resonant surface where the response was introduced, agreeing with results observed in sophisticated simulation codes [14], [15], [27], [29], [30]. We point out that relevant questions of particle transport [31] are not in the scope of this paper. Finally, for the considered perturbed large aspect ratio tokamak equilibrium, the number of toroidal turns, called connection lengths, performed by the perturbed magnetic field lines until reaching the tokamak wall are calculated, and the results indicate that the plasma response introduces a homogenization effect on the connection length distribution, revealing some insights regarding deposition patterns at the tokamak wall.

In Section II, the magnetohydrodynamical plasma equilibrium is presented for a large aspect ratio tokamak, and the associated magnetic field is modified in order to include a correction that mimics the curvature of the plasma axis in large aspect ratio tokamaks. In Section III, the RMPs equivalent to those introduced by resonant helical windings are presented. The modeling of the plasma response can be found in Section IV. Numerical results on our model with and without plasma response are presented in Section V. Connection length investigations are found in Section VI. Finally, conclusions are presented in Section VII.

II. Magnetohydrodynamical Equilibrium

The Grad–Shafranov equation in cylindrical coordinates (r, θ, z) can be written as [32]

$$\frac{1}{r}\frac{\partial}{\partial r}\left(r\frac{\partial \psi}{\partial r}\right) = \mu_0 J_z(\psi) \tag{1}$$

where ψ is the magnetic flux function and J_z is the current profile along a plasma cross section, which in this case is considered as

$$J_z(r) = \frac{4I_p}{\pi a^2}\left[1-\left(\frac{r}{a}\right)^2\right]^{\gamma} \tag{2}$$

with I_p representing the plasma current, a the plasma column radius, and $\gamma = 3$ a constant parameter. The large aspect ratio approximation was introduced here choosing a current density which only depends on r variable and represents a peaked current profile, commonly observed in tokamak discharges.

In cylindrical coordinates, the equilibrium magnetic field can be represented as $\vec{B}_0 = B_0^{\theta}\vec{e}_{\theta} + B_0^{z}\vec{e}_z$, such as $\vec{e}_z \times \vec{e}_r = \vec{e}_{\theta}/r$ and the components B_0^{θ} and B_0^{z} are expressed, respectively, in T/m and T. From (1) and (2), one can obtain the equilibrium magnetic field

$$\vec{B}_0 \cong \frac{\mu_0 I_p}{2\pi r^2}\left[1-\left(1-\frac{r^2}{a^2}\right)^{\gamma+1}\right]\vec{e}_{\theta} + \frac{\mu_0 I_e}{2\pi R_0}\vec{e}_z \tag{3}$$

where $2\pi R_0$ is the periodic length along the cylindrical plasma and I_e is the external current that generates the equilibrium toroidal field.

In order to mimic the curvature of the plasma axis in large aspect ratio tokamaks, regarding toroidal geometry effects, we modify the component B_0^z, so (3) can be written as [33]

$$\vec{B}_0 \cong \frac{\mu_0 I_p}{2\pi r^2}\left[1-\left(1-\frac{r^2}{a^2}\right)^{\gamma+1}\right]\vec{e}_{\theta} + \frac{\mu_0 I_e}{2\pi (R_0 + r\cos\theta)}\vec{e}_z. \tag{4}$$

The safety factor along a plasma cross section associated with the equilibrium magnetic field, shown in (4), is defined as [4]

$$q(r) = \frac{1}{2\pi R_0}\int_0^{2\pi}\frac{B_0^z}{B_0^{\theta}}d\theta = q_c(r)\frac{R_0}{\sqrt{R_0^2 - r^2}} \tag{5}$$

where $q_c(r) = B_0^z/(B_0^{\theta}R_0)$ represents the safety factor for a cylindrical plasma.

Equations (4) and (5) are valid for large aspect ratio tokamaks with a correction in the toroidal field. This approach introduces a poloidal angle dependence on the equilibrium magnetic surfaces. However, for numerical applications, parameters, and profiles as the safety factor, the magnetic field components and the plasma radii are chosen compatible with those typical of the tokamak TCABR, whose aspect ratio is 3.4. This approximation has been used in the literature for tokamaks such as TCABR, JET, and JT-60, (see [34]).

Fig. 1 shows the safety factor profile for the tokamak TCABR parameters [35]: $I_p = 70$ kA, $I_e = 4$ MA, $a = 0.18$ m, and $R_0 = 0.61$ m. The horizontal and vertical dotted lines emphasize the radial location related to $q = 4$, near the tokamak wall, where analyzes are performed. Since the plasma response to external perturbations of interest for the tokamak TCABR is studied in this paper, the same parameters used in Fig. 1 are employed to obtain the results of the following sections.

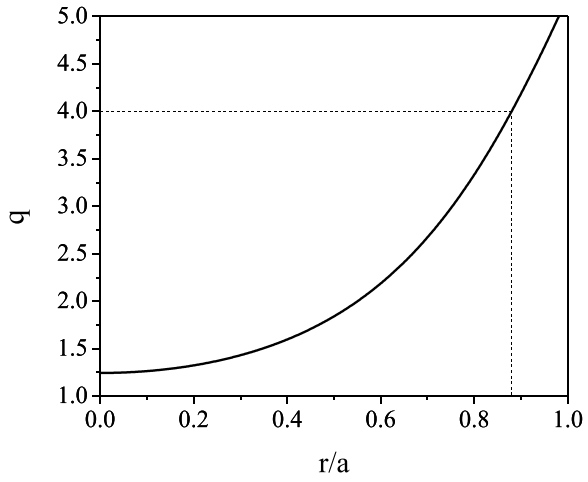

Fig. 1. Safety factor profile emphasizing the radial location related to $q = 4$, near the tokamak wall, where the numerical calculations are performed.

III. Resonant Magnetic Perturbations

In this paper, RMPs are included in order to create a layer of chaotic field lines near the tokamak wall. The RMPs are generated by two helical wires, placed on the external surface of the considered large aspect ratio tokamak, conducting currents in opposed directions and acting similar to an EML [4].

Since the external perturbation is composed by a pair of identical helices, it is convenient to define the variable $u_h = m_0\theta - n_0(z/R_0)$, where m_0 and n_0 are, respectively, the poloidal and toroidal mode numbers associated with the external helical windings. The set of points with u_h equal to a constant value is defined by the "winding law"

$$u_h = m_0\theta - n_0(z/R_0) = \text{constant}. \tag{6}$$

The current density, $\vec{J}_h$, associated with the pair of helices can be read as [4]

$$\vec{J}_h = I_{lh}\delta(r-b)[\delta(u_h - 0) - \delta(u_h - \pi)]\vec{e}_{\text{hel}} \tag{7}$$

where $I_{lh} = I_h/(2\pi b)$ is the perturbation linear density, $b = 0.22$ m is the cylinder radius, and the helical vector is defined as

$$\vec{e}_{\text{hel}} = \left[\alpha/\left(\sqrt{b^2\alpha^2+1}\right)\right]\vec{e}_\theta + \left[1/\left(\sqrt{b^2\alpha^2+1}\right)\right]\vec{e}_z \tag{8}$$

with $\alpha = B_0^\theta/B_0^z$.

The magnetic field component due to the helical wires can be represented as $\vec{B}_h(r,\theta,z) = \nabla\phi_h(r,\theta,z)$ and, since $\nabla\cdot\vec{B}_h(r,\theta,z) = 0$, the Laplace equation $\nabla^2\phi_h(r,\theta,z) = 0$ is solved in cylindrical coordinates in order to calculate the magnetic field due to the RMP.

The Laplace equation general solution in cylindrical coordinates is given by

$$\phi_h(r,\theta,z) = \sum_{k_z=-\infty}^{+\infty}\sum_{k_\theta=-\infty}^{+\infty} C_{k_z,k_\theta} I_{k_\theta}(k_z\beta r)e^{i(k_\theta\theta - k_z\beta z)} \tag{9}$$

where C_{k_z,k_θ} is calculated from the boundary conditions and $I_{k_\theta}(k_z\beta r)$ is the modified Bessel function of first kind.

IV. Plasma Response

In order to estimate the effects of plasma response in our model, following the idea from [14], which mimics the plasma response by introducing a helical current sheet to suppress magnetic islands at the resonant surface, the same analytical procedure presented in previous section is applied to calculate the magnetic field associated with a RMP composed by a single current sheet, located at the defined radial surface $r = r_0$. For this case, the current density is defined as

$$\vec{J}_{pr} = j\delta(r-r_0)\vec{e}_{\text{hel}} \tag{10}$$

where

$$j = \sum_{N=1}^{+\infty} j_N e^{iN(m_0\theta - n_0 z/R_0)}. \tag{11}$$

In order to obtain j_N, the plasma response condition $(\vec{B}_h + \vec{B}_{pr})\cdot\nabla r = 0$ is applied at $r = r_0$ [14]. Since $\vec{B}_h$ represents the magnetic field created by the pair of helices and $\vec{B}_{pr}$ represents the magnetic field created by the current sheet, the radial component of the resulting magnetic field vanishes at $r = r_0$.

The magnetic field created by the current sheet is calculated by $\vec{B}_{pr} = \nabla\phi_{pr}$, where the scalar field ϕ_{pr} is obtained by solving the Laplace equation $\nabla^2\phi_{pr}(r,\theta,z) = 0$, which provides the general solution

$$\phi_{pr}(r,\theta,z) = \begin{cases} \displaystyle\sum_{k_z=-\infty}^{+\infty}\sum_{k_\theta=-\infty}^{+\infty} C^i_{k_z,k_\theta} I_{k_\theta}(k_z\beta r)e^{i(k_\theta\theta - k_z\beta z)} & \text{if r} < \text{r}_0 \\ \displaystyle\sum_{k_z=-\infty}^{+\infty}\sum_{k_\theta=-\infty}^{+\infty} C^e_{k_z,k_\theta} K_{k_\theta}(k_z\beta r)e^{i(k_\theta\theta - k_z\beta z)} & \text{if r} > \text{r}_0 \end{cases} \tag{12}$$

where $C^i_{k_z,k_\theta}$ and $C^e_{k_z,k_\theta}$ are calculated from the boundary conditions and $I_{k_\theta}(k_z\beta r)$ and $K_{k_\theta}(k_z\beta r)$ are, respectively, the modified Bessel functions of the first and the second kind.

V. Numerical Results

In order to analyze how the plasma response modifies the magnetic field topology, the magnetic field line equation

$$(\vec{B}_0 + \vec{B}_h + \vec{B}_{pr})\times d\vec{l} = 0 \tag{13}$$

is solved numerically, where $d\vec{l}$ represents an infinitesimal displacement along the magnetic field lines. The RMP excites the main mode $(m,n) = (4,1)$ on the magnetic rational surface associated with the safety factor $q(r_0) = 4$, represented by the intersection of the dotted lines in Fig. 1. To present the magnetic configuration obtained from the mentioned integration, we follow the magnetic field lines for several chosen initial conditions and obtain the Poincaré maps, for $z = 0$, as those shown in Figs. 2 and 3.

Fig. 2(a) and (b) shows the Poincaré plots without plasma response for $I_h = 3.5$ kA, which corresponds to 5% of the plasma current, and for $I_h = 21$ kA, which corresponds to 30% of the plasma current and is very high from experimental point of view. However, due to simplifications associated with our cylindrical plasma model, which does not take into account

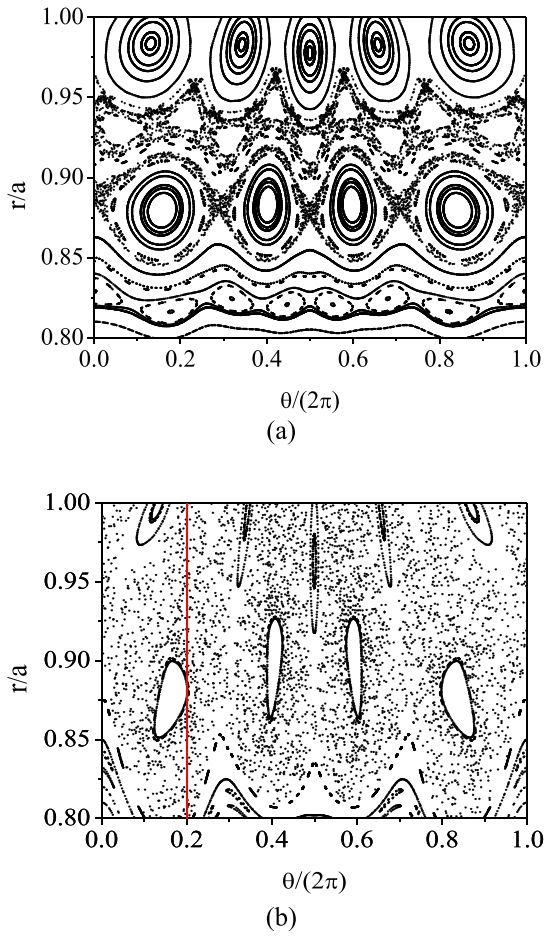

Fig. 2. Poincaré plots without plasma response for (a) $I_h = 3.5$ kA and (b) $I_h = 21$ kA. The red vertical line represents the set of points used to calculate the connection lengths in Section VI.

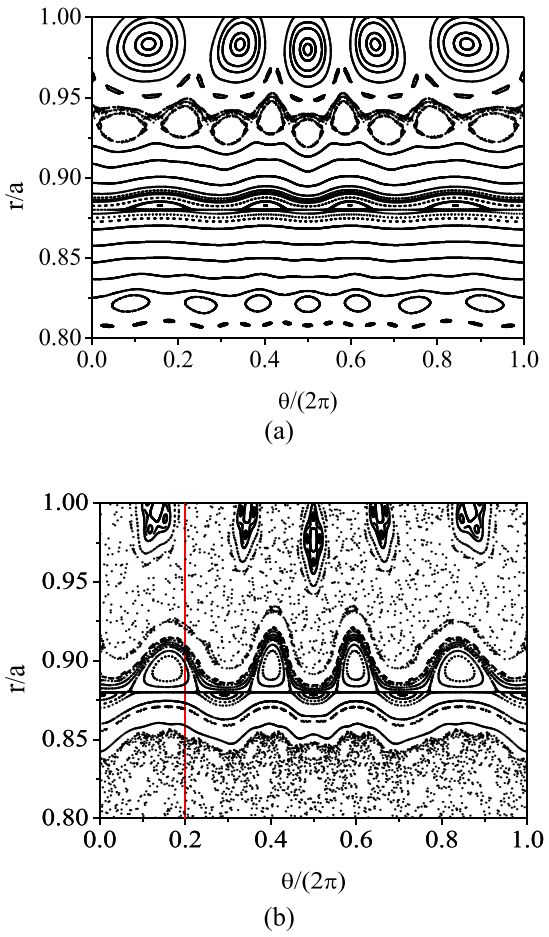

Fig. 3. Poincaré plots with plasma response for (a) $I_h = 3.5$ kA and (b) $I_h = 21$ kA. The red vertical line represents the set of points used to calculate the connection lengths in Section VI.

Shafranov shift, only small correction effects in toroidal field, [see (4)], in comparison to tokamaks, we have to adopt this high value to show chaos around the magnetic islands. As we are interested in studying escaping pattern near the wall, our approach still remains valid. Since chaotic magnetic field lines have profound implications for the plasma confinement in tokamaks [14], [15] and as our goal is to study the escape channels through the connection lengths, we adopt this high value for the perturbation current. Considering $\delta B_{h,r}$ the amplitude of the r component of the perturbative field and $\bar{B}_{0,z}$ the mean z component of the equilibrium magnetic field given by (4), both calculated for $r_0/a \cong 0.88$, the ratio $\delta B_{h,r}/\bar{B}_{0,z}$ can be estimated for perturbation parameters $I_h = 3.5$ kA and $I_h = 21$ kA, resulting in $\delta B_{h,r}/\bar{B}_{0,z} \cong 2.1 \times 10^{-4}$ and $\delta B_{h,r}/B_{0,z} \cong 1.3 \times 10^{-3}$, respectively. Although these perturbation currents are considered high for experimental studies, the magnitude of $\delta B_{h,r}/\bar{B}_{0,z}$ is similar to the RMP studies conducted in the TEXT tokamak [10]. Fig. 2(a) shows the main island chain $(m, n) = (4, 1)$, located at the perturbed resonant surface, $r_0/a \cong 0.88$, generated by the RMP. One can notice a secondary island chain with $(m, n) = (5, 1)$, located near the plasma edge $r/a = 1$, which is a result of the toroidal correction, applied in (4) [36]. Sets of smaller islands can also be found surrounding the islands $(4, 1)$ and $(5, 1)$, as well as regular magnetic surfaces and chaotic magnetic field lines. By increasing the perturbation current to $I_h = 21$ kA, as represented in Fig. 2(b), one can notice larger chaotic regions, especially around the islands $(4, 1)$ and $(5, 1)$, produced by the breakup of regular magnetic surfaces and small islands.

Fig. 3(a) and (b) shows the Poincaré plots with plasma response for $I_h = 3.5$ kA and $I_h = 21$ kA, respectively. Following [14], the plasma response is modeled as an RMP, composed by a current sheet at the radial position of the main resonant mode $(4, 1)$, $r_0/a \cong 0.88$, and it eliminates the total radial component of the magnetic field at $r = r_0$. The elimination of the total radial magnetic component introduces a horizontal straight line at $r/a \cong 0.88$ crossing the main resonant mode $(4, 1)$, causing topological rearrangements on the Poincaré plots. This corresponds to a robust torus similar to those introduced in [37] and [38].

When comparing Fig. 2(a) with Fig. 3(a), as well as Fig. 2(b) with Fig. 3(b), we notice the duplication on the number of islands surrounding $r/a \cong 0.88$, in which instead of four, now there are eight magnetic islands. This duplication effect is barely seen in Fig. 3(a), being clearer in Fig. 3(b), and can be related to a bifurcation of hyperbolic fixed points (X-points), on the presence of a robust torus, i.e., an invariant surface with a null magnetic field radial component on

the surface with a perturbing plasma current. Around the robust torus invariant surfaces are created, stabilizing the plasma and decreasing the transport [37], [38]. One can also notice the regularization of chaotic structures around the straight line, $r/a \cong 0.88$, and the decrease in the magnetic islands width. These effects reported in here were emphasized in previous works using sophisticated simulation codes [14], [15], [27], [29], [30]. Although the plasma response creates a transport barrier on the resonant surface (4, 1), we still note in Fig. 3(a) and (b) secondary islands that deteriorate the plasma confinement, but do not affect the transport around the primary resonant surface. Secondary islands, as already mentioned, appear due to the effects of the toroidicity of the magnetic field.

VI. Connection Length and Escape Patterns

The numbers of toroidal turns performed by magnetic field lines until reaching the tokamak wall are called connection lengths and, since particles follow magnetic field lines, their distributions directly interfere on the heat flux transport, determining the deposition patterns on plasma facing components [39]. Accordingly, we consider our model to calculate the escape of field lines by integrating initial conditions in a box with $0 \leq \theta/2\pi \leq 1$ and $0.8 \leq r/a \leq 1$, followed by the construction of a color map, where the color indicates the number of toroidal turns that the field line needs to reach the tokamak wall, located at $r = b$. The concept of toroidal turns for a cylindrical geometry regards the number of times that the field line travels the distance $2\pi R_0$, along the plasma axis, until it reaches the wall. Field lines with 1000 or more toroidal turns are considered trapped on regular surfaces or islands.

Fig. 4(a) and (b) shows the connection length distribution for $I_h = 21$ kA without and with plasma response, respectively. In order to analyze escape patterns, a perturbation strong enough to break most regular magnetic surfaces and islands on phase space is required, so the field lines will have escaping channels to reach the tokamak wall. Due to the cylindrical geometry of our model, in order to achieve such scenario, the perturbation parameter has to be set to values considerably greater than the ones commonly used for EMLs, as we have previously justified. Then, the perturbation current was defined as $I_h = 21$ kA, which corresponds to 30% of the plasma current, so that most regular magnetic surfaces on phase space are broken and the plasma response model can be fully analyzed.

Fig. 4(a) shows the connection lengths distribution corresponding to the Poincaré section from Fig. 2(b), without plasma response. The red regions represent the magnetic field lines trapped on regular surfaces or islands. The blue regions correspond to field lines escaping with just a few toroidal turns, and these field lines are most likely to be located near or on manifolds of homoclinic tangles [40]. Fig. 4(b) shows the connection lengths distribution corresponding to the Poincaré section from Fig. 3(b), with plasma response. The wide red region, located in the interval $0.80 \leq r/a \leq 0.90$, represents a significant amount of field lines that are trapped on phase space due to the introduction of the plasma response, in comparison

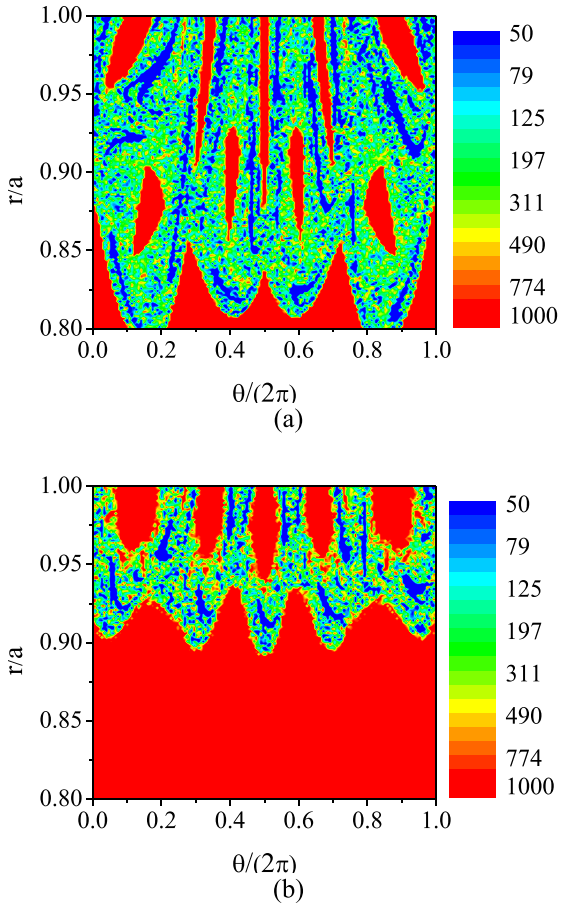

Fig. 4. Connection lengths for $I_h = 21$ kA. (a) Without plasma response. (b) With plasma response.

to Fig. 4(a), which is an indicative of the regularization of chaotic structures around $r/a \cong 0.88$, as previously observed in Fig. 3(b). This effect was also observed with 3-D computer simulations for the DIII-D tokamak [15].

Fig. 5(a) shows the connection lengths related to the reference line (in red) from Fig. 2(b), without plasma response. The plateau in the region $0.85 \leq r/a \leq 0.90$ indicates field lines trapped on the edge of an island [see Fig. 2(b) for more details], while the plateau in the region $0.95 \leq r/a \leq 1.00$ indicates field lines escaping with only few toroidal turns, most likely to be located near or on manifolds of homoclinic tangles [40] [see Fig. 4(a) for more details].

Fig. 5(b) shows the connection lengths related to the reference line (in red) from Fig. 3(b), with plasma response. The wide plateau, in the interval $0.80 \leq r/a \leq 0.90$, indicates field lines trapped on regular surfaces or islands, caused by the introduction of the plasma response, due to the regularization of chaotic structures around $r/a \cong 0.88$ (see Figs. 3(b) and 4(b) for more details).

Fig. 6 shows the histogram composed by the connection lengths from Fig. 5, for the cases without plasma response (in blue), from Fig. 5(a), and with plasma response (in red), from Fig. 5(b). The tall red bar shows that almost 65% of the field lines are trapped on regular surfaces or islands, caused by the introduction of the plasma response, due to the regularization of chaotic structures around $r/a \cong 0.88$, while

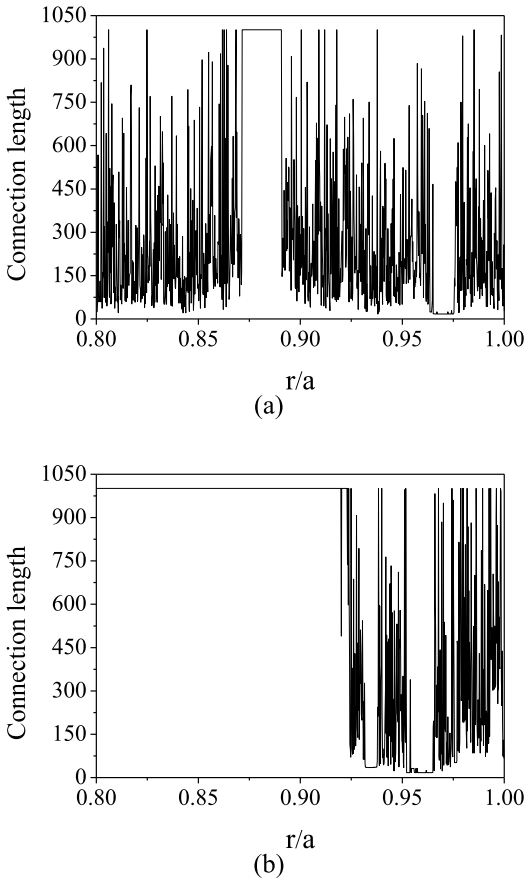

Fig. 5. Connection lengths for magnetic field lines located on the reference line (in red) from (a) Fig. 2(b), without plasma response and (b) Fig. 3(b), with plasma response.

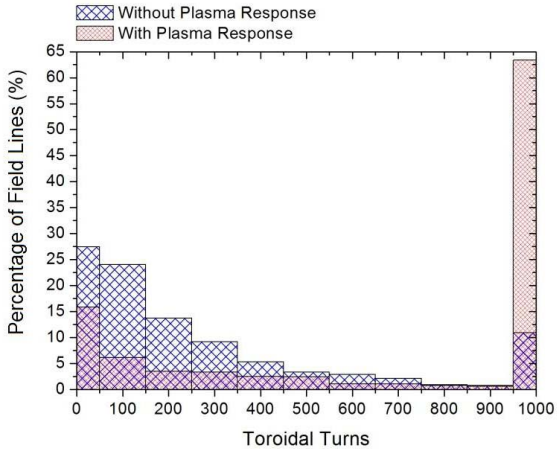

Fig. 6. Histogram, from Fig. 5, emphasizing the percentage of escaping lines versus the number of toroidal turns performed to escape, for the cases without plasma response (in blue) and with plasma response (in red).

approximately only 35% of the field lines escape with less than 1000 toroidal turns. However, without plasma response (blue bars), almost 11% of the field lines are considered trapped escaping with 1000 or more toroidal turns, and 89% of the field lines escape with less than 1000 toroidal turns. One can also notice that, without plasma response, there are widely different percentages of escaping lines, located mostly between 0% and 30%, for different toroidal turns. Furthermore, with plasma response (red bars), we find escaping lines between 0% and 5% for different toroidal turns, indicating that the introduction of plasma response also causes a homogenization effect on the connection lengths distribution, when compared to the case without plasma response.

VII. Conclusion

This paper has presented a plasma model for large aspect ratio tokamaks, whose equilibrium was modified to mimic the curvature of the plasma axis, on the presence of RMPs created by resonant helical windings, similar to those introduced by an EML. The helical windings located on the external wall of the tokamak generate a perturbation in an equilibrium magnetic surface. The plasma response is modeled as a RMP created by a current sheet such that the radial component of the total magnetic field at the perturbed surface vanishes.

After solving numerically the magnetic field line differential equations, the influence of the plasma response on the field line topology can be observed due to the reduction of magnetic island sizes and the regularization of chaotic regions around the resonant surface where the response was introduced, agreeing with results observed in sophisticated simulation codes.

The effect of plasma response on the numbers of toroidal turns, called connection lengths, performed by magnetic field lines until reaching the tokamak wall also indicates that the number of trapped field lines is increased on the phase space, which is an effect also observed in previous works with 3-D computer simulations for the DIII-D tokamak.

A homogenization effect on the connection length distribution, introduced by the plasma response, was also reported, revealing some insights regarding deposition patterns at the tokamak wall.

References

[1] G. M. McCracken and P. E. Stott, "Plasma-surface interactions in tokamaks," *Nucl. Fusion*, vol. 19, no. 7, pp. 889–981, Jul. 1979.

[2] R. Parker *et al.*, "Plasma-wall interactions in ITER," *J. Nucl. Mater.*, vols. 241–243, pp. 1–26, Feb. 1997.

[3] P. Ghendrih, A. Grosman, and H. Capes, "Theoretical and experimental investigations of stochastic boundaries in tokamaks," *Plasma Phys. Controlled Fusion*, vol. 38, no. 10, pp. 1653–1724, Oct. 1996.

[4] E. C. D. Silva, I. L. Caldas, and R. L. Viana, "The structure of chaotic magnetic field lines in a tokamak with external nonsymmetric magnetic perturbations," *IEEE Trans. Plasma Sci.*, vol. 29, no. 4, pp. 617–631, Aug. 2001.

[5] M. Lehnen *et al.*, "First results from the dynamic ergodic divertor at TEXTOR," *J. Nucl. Mater.*, vols. 337–339, pp. 171–175, Mar. 2005.

[6] R. A. Moyer *et al.*, "Edge localized mode control with an edge resonant magnetic perturbation," *Phys. Plasmas*, vol. 12, no. 5, p. 056119, Apr. 2005.

[7] K. H. Finken *et al.*, "Influence of the dynamic ergodic divertor on transport properties in TEXTOR," *Nucl. Fusion*, vol. 47, no. 7, pp. 522–534, Jul. 2007.

[8] F. Karger and K. Lackner, "Resonant helical divertor," *Phys. Lett. A*, vol. 61, no. 6, pp. 385–387, Jun. 1977.

[9] M. Roberto, E. C. da Silva, I. L. Caldas, and R. L. Viana, "Magnetic trapping caused by resonant perturbations in tokamaks with reversed magnetic shear," *Phys. Plasmas*, vol. 11, no. 1, pp. 214–225, Jan. 2004.

[10] T. E. Evans, "Resonant magnetic perturbations of edge-plasmas in toroidal confinement devices," *Plasma Phys. Controlled Fusion*, vol. 57, no. 12, p. 123001, Nov. 2015.

[11] S. Abdullaev, "Magnetic field of resonant magnetic perturbations," in *Magnetic Stochasticity in Magnetically Confined Fusion Plasmas*, 1st ed. Berlin, Germany: Springer, 2014, pp. 227–262.

[12] O. Schmitz *et al.*, "Resonant pedestal pressure reduction induced by a thermal transport enhancement due to stochastic magnetic boundary layers in high temperature plasmas," *Phys. Rev. Lett.*, vol. 103, no. 16, p. 165005, Oct. 2009.
[13] A. Wingen *et al.*, "Connection between plasma response and resonant magnetic perturbation (RMP) edge localized mode (ELM) suppression in DIII-D," *Plasma Phys. Controlled Fusion*, vol. 57, no. 10, p. 104006, Sep. 2015.
[14] P. Cahyna, E. Nardon, and J. E. Contributors, "Model for screening of resonant magnetic perturbations by plasma in a realistic tokamak geometry and its impact on divertor strike points," *J. Nucl. Mater.*, vol. 415, no. 1, pp. S927–S931, Aug. 2011.
[15] H. Frerichs *et al.*, "Impact of screening of resonant magnetic perturbations in three dimensional edge plasma transport simulations for DIII-D," *Phys. Plasmas*, vol. 19, no. 5, p. 052507, May 2012.
[16] F. L. Waelbroeck, I. Joseph, E. Nardon, M. Bécoulet, and R. Fitzpatrick, "Role of singular layers in the plasma response to resonant magnetic perturbations," *Nucl. Fusion*, vol. 52, no. 7, p. 074004, Jul. 2012.
[17] J.-K. Park, A. H. Boozer, and A. H. Glasser, "Computation of three-dimensional tokamak and spherical torus equilibria," *Phys. Plasmas*, vol. 14, no. 5, p. 052110, May 2007.
[18] Y. Liu, A. Kirk, Y. Gribov, M. P. Gryasnevich, T. C. Hender, and E. Nardon, "Modelling of plasma response to resonant magnetic perturbation fields in MAST and ITER," *Nucl. Fusion*, vol. 51, no. 8, p. 083002, Aug. 2011.
[19] M. Bécoulet *et al.*, "Physics of penetration of resonant magnetic perturbations used for type I edge localized modes suppression in tokamaks," *Nucl. Fusion*, vol. 49, no. 8, p. 085011, Aug. 2009.
[20] Y. Yang *et al.*, "Experimental observations of plasma edge magnetic field response to resonant magnetic perturbation on the TEXTOR tokamak," *Nucl. Fusion*, vol. 52, no. 7, p. 074014, Jul. 2012.
[21] A. J. Thornton *et al.*, "The effect of resonant magnetic perturbations on the divertor heat and particle fluxes in MAST," *Nucl. Fusion*, vol. 54, no. 6, p. 064011 Jun. 2014.
[22] Y. Suzuki *et al.*, "3D plasma response to the magnetic field structure in the large helical device," *Nucl. Fusion*, vol. 53, no. 7, p. 073045, Jul. 2013.
[23] I. Joseph, "Edge-localized mode control and transport generated by externally applied magnetic perturbations," *Contrib. Plasma Phys.*, vol. 52, nos. 5–6, pp. 326–347, Jun. 2012.
[24] T. E. R. A. Evans Moyer *et al.*, "Suppression of large edge localized modes with edge resonant magnetic fields in high confinement DIII-D plasmas," *Nucl. Fusion*, vol. 45, no. 7, pp. 595–607, Jun. 2005.
[25] M. F. Heyn, I. B. Ivanov, S. V. Kasilov, and W. Kernbichler, "Kinetic modelling of the interaction of rotating magnetic fields with a radially inhomogeneous plasma," *Nucl. Fusion*, vol. 46, no. 4, pp. S159–S169, Apr. 2006.
[26] D. Ciro, T. E. Evans, and I. L. Caldas, "Modeling non-stationary, non-axisymmetric heat patterns in DIII-D tokamak," *Nucl. Fusion*, vol. 57, no. 1, p. 016017, Jan. 2017.
[27] Y. Liu *et al.*, "ELM control with RMP: Plasma response models and the role of edge peeling response," *Plasma Phys. Control. Fusion*, vol. 58, no. 11, p. 114005, Oct. 2016.
[28] P. Cahyna *et al.*, "Strike point splitting induced by the application of magnetic perturbations on MAST," *J. Nucl. Mater.*, vol. 438, pp. S326–S329, Jul. 2013.
[29] Y. Liu, A. Kirk, and Y. Sun, "Toroidal modeling of penetration of the resonant magnetic perturbation field," *Phys. Plasmas*, vol. 20, no. 4, p. 042503, Apr. 2013.
[30] F. Orain *et al.*, "Non-linear modeling of the plasma response to RMPs in ASDEX upgrade," *Nucl. Fusion*, vol. 57, no. 2, p. 022013, Sep. 2017.
[31] V. Rozhansky, "Drifts, currents, and radial electric field in the edge plasma with impact on pedestal, divertor asymmetry and RMP consequences," *Contrib. Plasma Phys.*, vol. 54, nos. 4–6, pp. 508–516, Jun. 2014.
[32] M. Y. Kucinski, I. L. Caldas, L. H. A. Monteiro, and V. Okano, "Toroidal plasma equilibrium with arbitrary current distribution," *J. Plasma Phys.*, vol. 44, no. 2, pp. 303–311, Oct. 1990.
[33] J. M. Finn, "The destruction of magnetic surfaces in tokamaks by current perturbations," *Nucl. Fusion*, vol. 15, no. 5, pp. 845–854, Oct. 1975.
[34] K. Nishikawa and M. Wakatani, "Progress in fusion research," in *Plasma Physics*, 3rd ed. Berlin, Germany: Springer, 2000, pp. 282–297.
[35] E. C. da Silva, I. L. Caldas, and R. L. Viana, "Ergodic magnetic limiter for the TCABR," *Brazilian J. Phys.*, vol. 32, no. 1, pp. 39–45, Mar. 2002.
[36] A. C. Fraile, Jr., M. Roberto, and I. L. Caldas, "Plasma response in cylindrical tokamaks," in *Proc. 6th Int. Conf. Nonlinear Sci. Complex.*, São José dos Campos, Brazil, May 2016, doi: 10.20906/CPS/NSC2016-0069.
[37] R. Egydio de Carvalho, C. G. L. Martins, and G. M. Favaro, "Interference of robust tori on the resonance overlap," *Brazilian J. Phys.*, vol. 39, no. 3, pp. 606–614, Sep. 2009.
[38] R. Egydio de Carvalho and G. M. Favaro, "The defocusing mechanism of isochronous resonances," *Phys. A, Stat. Mech. Appl.*, vol. 350, nos. 2–4, pp. 173–182, May 2005.
[39] T. E. Evans, R. A. Moyer, and P. Monat, "Modeling of stochastic magnetic flux loss from the edge of a poloidally diverted tokamak," *Phys. Plasmas*, vol. 9, no. 12, p. 4957, Dec. 2002.
[40] C. G. L. Martins, M. Roberto, and I. L. Caldas, "Delineating the magnetic field line escape pattern and stickiness in a poloidally diverted tokamak," *Phys. Plasmas*, vol. 21, no. 8, p. 082506, Aug. 2014.

André Carlos Fraile Jr. received the B.Sc. degree in aeronautical engineering and the M.Sc. degree in physics from the Aeronautics Institute of Technology, São José dos Campos, Brazil, in 2008 and 2012, respectively, where he is currently pursuing the Ph.D. degree in plasma physics.

Since 2009, he has been with the Institute for Advanced Studies, São José dos Campos. His current research interests include plasma physics and computational fluid dynamics applied to high-speed flows.

Marisa Roberto received the B.S. degree in physics from the Catholic University of São Paulo, São Paulo, Brazil, in 1982, the M.S. degree from the Space Research Institute, São Jose dos Campos, Brazil, in 1986, and the Ph.D. degree in plasma physics from the Aeronautics Institute of Technology (ITA), in São Jose dos Campos, in 1992.

From 1999 to 2004, she was a Visiting Scholar with the University of California at Berkeley, Berkeley, CA, USA. She is currently a Full Professor with the Physics Department, ITA. Her current research interests include plasma physics for technological applications and chaos.

Iberê Luiz Caldas was born in Santos, Brazil, in 1948. He received the B.S. and Ph.D. degrees in physics from the Institute of Physics, University of São Paulo (IF-USP), São Paulo, Brazil, in 1970 and 1979, respectively.

In 1977, 1979, 1983, 1984, and 1988, he was a Guest Scientist with the Max-Planck-Institut fuer PlasmaPhysik, Garching bei München, Germany. Since 1995, he has been a Full Professor with IF-USP. His current research interests include plasma physics and chaos.

Caroline Gameiro Lopes Martins was born in São Paulo, Brazil, in 1986. She received the B.S. degree in physics from the Physics Department, São Paulo State University, Rio Claro, Brazil, in 2009, and the Ph.D. degree in physics from the Aeronautics Institute of Technology, São José dos Campos, Brazil, in 2013, respectively.

In 2014, she joined the Aeronautics Institute of Technology as a Post-Doctoral Researcher. She has been pursuing a career in culinary arts.